CERN-ACC-NOTE-2020-0070

Measurements of the Dielectric Properties of a Ferroelectric Ceramic for Use in a Fast Reactive Tuner

B. Freemire

Euclid Techlabs

November 2020

Contents

1 Executive Summary

A FerroElectric Fast Reactive Tuner (FE-FRT) for superconducting radio frequency cavities offers several advantages over conventional mechanical tuners, including faster reaction time, no moving parts, and a wide tuning range. Additionally, a FE-FRT presents the potential to save RF power that is typically wasted by overcoupling the SRF cavities. The realization of a FE-FRT depends on a ferroelectric material with sufficient large tunability and small loss. Recently, the first demonstration of a FE-FRT tuner was completed at CERN [1]. These encouraging results open the door to applying this technology to a wide range of tuners, including those for the 80 MHz cavities in the CERN-PS. To direct the technical design of such a tuner, the dielectric properties of the ferroelectric material should be measured in an appropriate frequency range. This technical note presents the measurements of the dielectric properties (relative permittivity and loss tangent) of a ferroelectric composite ceramic based on barium strontium titanate with magnesium-based additives near 80 MHz. The dielectric constant is found to be temperature dependent, with a value of 159.9±0.6 at 22° C. The loss tangent is independent of temperature, and found to be $(3.01\pm0.12) \times 10^{-4}$ in the 80 MHz frequency range.

2 Measurement Device Design

The physics goals driving the design of the measurement device were to make the structure resonant as close to 80 MHz as possible with the existing ferroelectric tubes, and to minimize surface and contact losses as to maximize the quality factor. The main practical considerations were finding a material supplier that could provide a metal tube of sufficient size and a machine shop that had the capabilities of machining the tube to the desired specifications and tolerances, while staying within the project budget.

The required size of a simple pillbox resonant at 80 MHz is too large to be practical, so a reentrant design was adopted. The estimated relative permittivity of the ferroelectric is 150, and the dimensions of the two tubes are given in Table 1. An aluminum pipe of sufficient diameter (254 mm, 10 inches) and length (609.6 mm, 24 inches) was available from Online Metals [2], and Xometry [3] was contracted to machine the metal components. Figure 1 shows a cross sectional view of the resonator. Shallow counterbores were added to the top and bottom plates to locate the inner conductor and ferroelectric tube. Coupling loops were placed on the top plate. Sixteen screws connect the top and bottom plates.

Table 1: Ferroelectric tube dimensions.

	Length [mm]	Inner Diameter [mm]	Inner Diameter [mm]
Tube 1	31.803	26.995	16.865
Tube 2	31.795	27.015	16.925

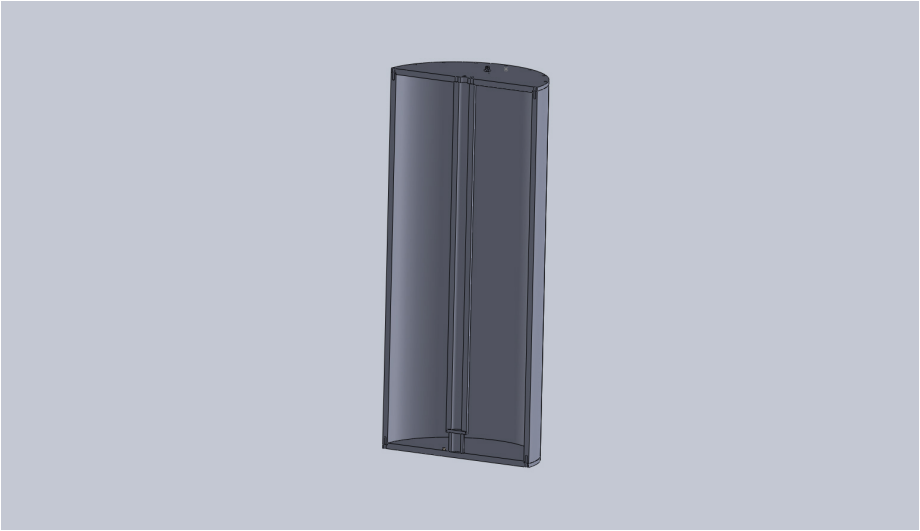

Figure 1: Cross sectional view of the resonator with the ferroelectric tube (bottom) and one coupling loop connector (top) shown.

The simulated lowest order mode of the structure based on the aluminum pipe and ferroelectric tube with a 38.1 mm (1.5 inches) inner conductor diameter is 71.837 MHz. Figure 2 shows the electric and magnetic field distributions based on an estimated dielectric constant of 150 for the ferroelectric tube.

3 Ferroelectric Tube Preparation

The ends of the ferroelectric tubes were sputtered with 700-800 nm of copper to reduce contact losses between the ceramic and metal. Figure 3 shows one of the tubes after sputtering. A cleaning procedure was performed both before and after sputtering. This procedure included wiping the tube with alcohol, rinsing with water, and placing the tube in a 2% Citranox solution. Before sputtering, the tube-Citranox solution was put in a sonicator and run at 55°C for five minutes. After sputtering, the sonicator was not used; the tube only sat for five minutes. The tube was then rinsed, blown dry with ultra-high purity nitrogen, baked in a furnace at 100°C for an hour, then stored in a desiccator until it was used.

4 Resonator Fabrication and Assembly

To improve the quality factor of the resonator, all aluminum surfaces were plated with silver with a minimum thickness of 7.62 μm (the skin depth of silver at 80 MHz is 7.09 μm) by Nobert Plating Company [4]. Figures 4 and 5 show

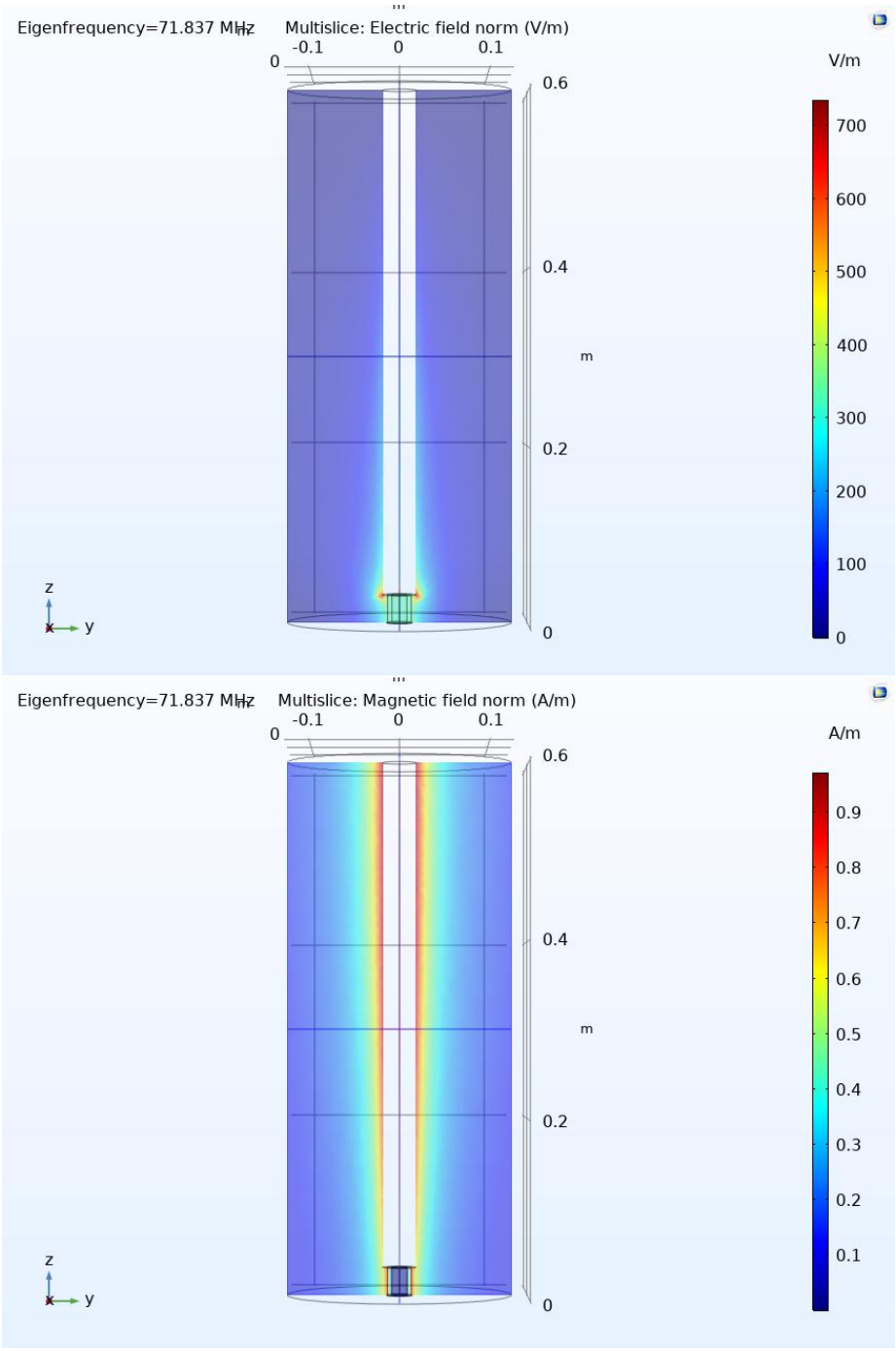

Figure 2: Electric (top) and magnetic (bottom) field distributions for the lowest order mode of the measurement device.

Figure 3: A ferroelectric tube after the ends were sputtered with copper.

photos of the aluminum components before and after silver plating.

An alignment jig was fabricated to ensure the inner conductor is parallel with the center axis of the resonator. A photo of the jig is shown in Figure 6. During assembly, the outer conductor was set on the jig using the dowel pins in the jig, the inner conductor was loosely screwed to the top plate, and top plate was tightly screwed to the outer conductor. The end of the inner conductor was captured in the conical section of the jig, and finally the screws holding the inner conductor to the top plate were tightened. The jig was then removed and the bottom plate attached.

5 Temperature Measurement and Calibration

As the dielectric constant of the ferroelectric material was believed to be highly temperature dependent, the temperature of each tube was recorded each time a measurement was made. It was not feasible to directly measure the temperature of the tube when measurements using a network analyzer were being made. Instead, the temperature of the tube was inferred by tracking the temperature of the cap on the inner conductor as a function of tube temperature prior the RF measurements. Two identical type K thermocouples were used, made of nickel, with an exposed probe tip and an accuracy of $\pm 0.50\%$ [5]. Figure 7 shows photos of the structure during thermocouple attachment and assembly. One thermocouple was attached to the surface of the inner conductor cap opposite of the ferroelectric tube using epoxy (Fig. 7, top left). The cap was then press fit into the end of the inner conductor. The other thermocouple was taped to

Figure 4: Aluminum outer conductor (left), bottom plate (right, top), and inner conductor (right, bottom) after machining.

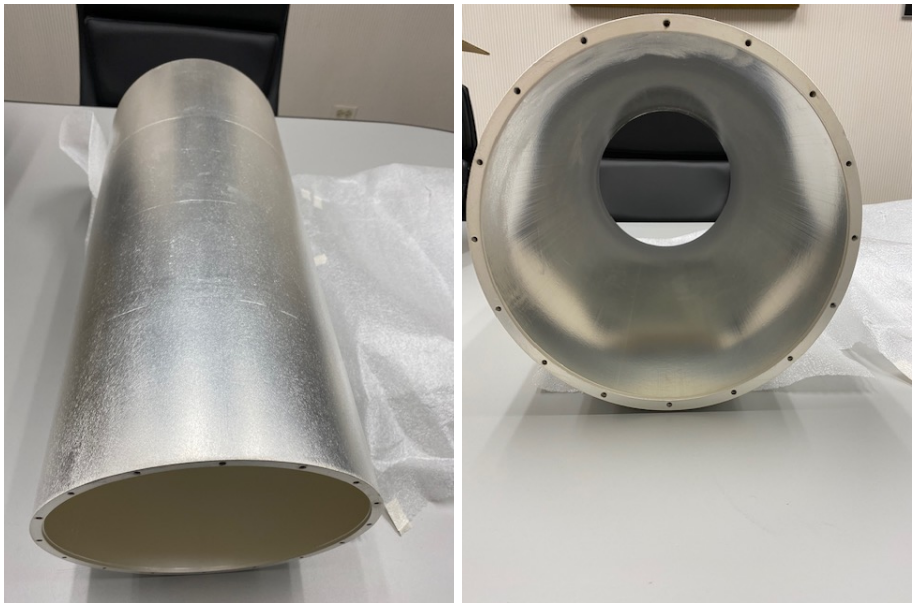

Figure 5: Aluminum outer conductor after being plated with silver.

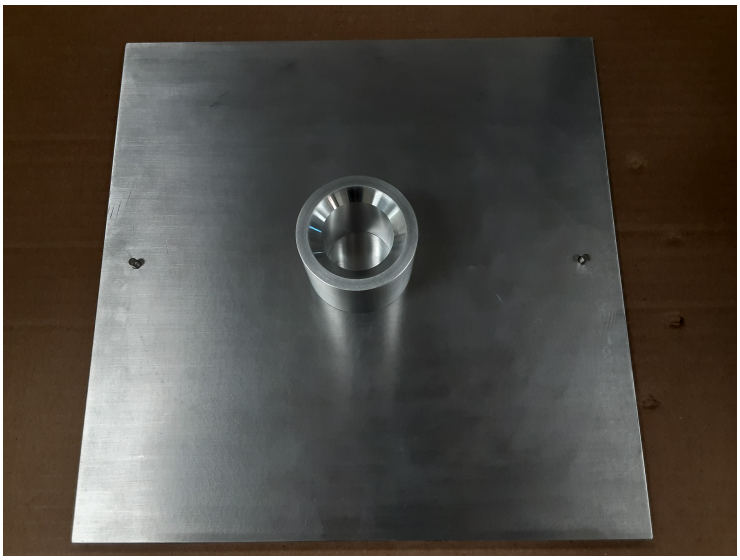

Figure 6: The jig used for aligning the inner conductor.

the outer surface of the tube and run through a penetration in the bottom plate (Fig. 7, top right).

Heat tape was wrapped around the exterior of the resonator. The potential applied to the heat tape was increased by 5 V, then the system was allowed to equilibrate for five minutes before the temperatures of the ferroelectric tube and inner conductor cap were recorded. Table 2 lists the calibration data and Figure 8 plots the data with a linear fit. For temperatures close to room temperature (e.g. $\leq$23.1°C), there is a simple offset of 0.2°C between the tube and cap temperatures.

6 Simulation Model Calibration

The internal dimensions of the resonator and effective surface conductivity of the silver were determined by assembling and measuring the empty structure, then adjusting the simulation parameters so that the simulated results matched those measured. Calipers were used to measure the component dimensions; a 6 inch (152.4 mm) maximum length set for small dimensions and 24 inch (609.6 mm) set for large dimensions. The outer conductor length, specified to be 24 inches, is the largest dimension and therefore this measurement will have the greatest uncertainty. The dimensions are listed in Table 3. The average values were used in the simulation model.

The top and bottom plates were turned down, as well as the ends of the outer conductor, to allow for alignment while assembling and increased contact between the components. This is shown in Figure 9. The value given for the

Figure 7: The thermocouple epoxied to the inner conductor cap (left, top), the ferroelectric tube with a thermocouple taped to it (right, top), and the resonator assembled for thermocouple calibration - photo (left, bottom) and diagram showing thermocouple cables and temperature readout (right, bottom).

Table 2: Temperature calibration data.

Time [min.]	Voltage [V]	Inner Cond. Temp. [°C]	Ceramic Temp. [°C]
0	0	22.8	23.0
5	5	22.9	23.1
10	10	23.0	23.2
15	15	23.1	23.3
20	20	23.1	23.5
25	25	23.2	23.8
30	30	23.3	24.4
35	35	23.5	25.1
40	40	23.8	26.2
45	45	24.2	27.7
50	50	24.8	29.3
55	55	25.5	31.3
60	60	26.7	33.9
65	65	28.0	36.9
70	70	29.7	39.9

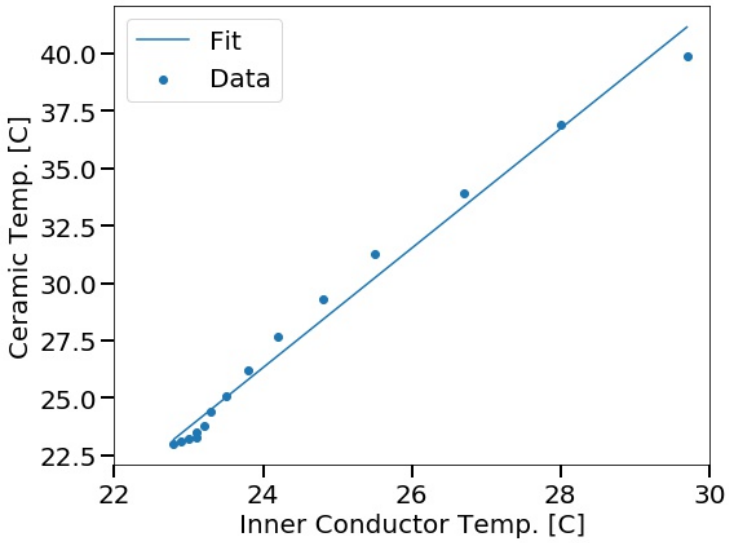

Figure 8: Ferroelectric tube temperature vs. inner conductor cap temperature. A linear fit has been applied to the data.

Table 3: Measured dimensions of the resonator components.

	Meas. [mm]	Avg. [mm]
Outer conductor ID, top	254.05	
	254.38	
	254.02	254.15
Outer conductor ID, bottom	252.88	
	255.05	
	255.10	254.34
Outer conductor length	611.64	611.64
Outer conductor top turndown depth	3.34	
	3.33	
	3.30	3.32
Outer conductor bottom turndown depth	3.33	
	3.35	
	3.44	3.37
Top plate turndown depth	3.07	
	3.09	
	3.13	3.10
Top plate counterbore diameter	39.56	39.56
Top plate counterbore depth	0.86	
	0.78	
	0.83	0.82
Bottom plate turndown depth	3.10	
	3.14	
	3.13	3.12
Bottom plate counterbore diameter	28.64	28.64
Bottom plate counterbore depth	0.81	
	0.77	
	0.86	0.81
Inner conductor diameter	38.11	
	38.11	
	38.10	38.11
Inner conductor length	573.44	
	573.54	573.49

outer conductor length in Table 3 includes the depth of the turndowns on both ends.

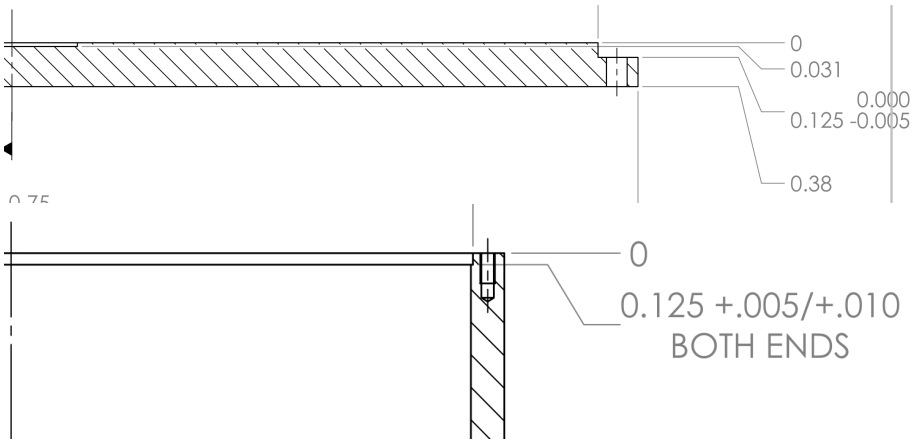

Figure 9: Drawings of the bottom plate (top) and outer conductor (bottom) showing the turndowns.

The diameters of the top and bottom of the outer conductor are not equal, and the bottom is more ovular than the top. The outer conductor in the simulation model was constructed by creating two ellipses, representing the top and bottom of the resonator, with major and minor diameters of the maximum and minimum dimensions listed in Table 3 for the top and bottom outer conductor inner diameters, separating them by the length of the outer conductor, then extruding each ellipse so that a continuous, smooth three dimensional semi-cylindrical volume was created.

The sum of the lengths of the ceramic tube and inner conductor must equal the sum of the depths of the counterbores in the top and bottom plates and distance between top and bottom plate faces - effectively the length of the outer conductor minus the turndowns on both ends, henceforth called the ***resonator length***. The lengths of the ceramic tube and counterbore depths were fixed in the simulation model.

Figure 10 shows photos taken during measurements of the empty resonator. Table 4 gives the measured data for the empty resonator, the simulated values based on the measured dimensions from Table 3 and a silver conductivity of 61.6×10^6 S/m, and the corrected simulated values. A dielectric constant of 1.00059 was used for air in the simulation model [6]. To match the frequency, the lengths of the resonator and inner conductor were adjusted. This resulted in corrected values of 573.48 mm for the inner conductor length, and 603.65 mm for the resonator length. The corrected value of the inner conductor is 0.01 mm smaller than the average measured value of 573.49 mm listed in Table 3. The corrected value of the resonator length is 1.30 mm (0.21%) smaller than the value of 604.95 mm based on the measurements in Table 3. The effective conductivity

of silver is 49.15×10^6 S/m to match the measured Q of the resonator.

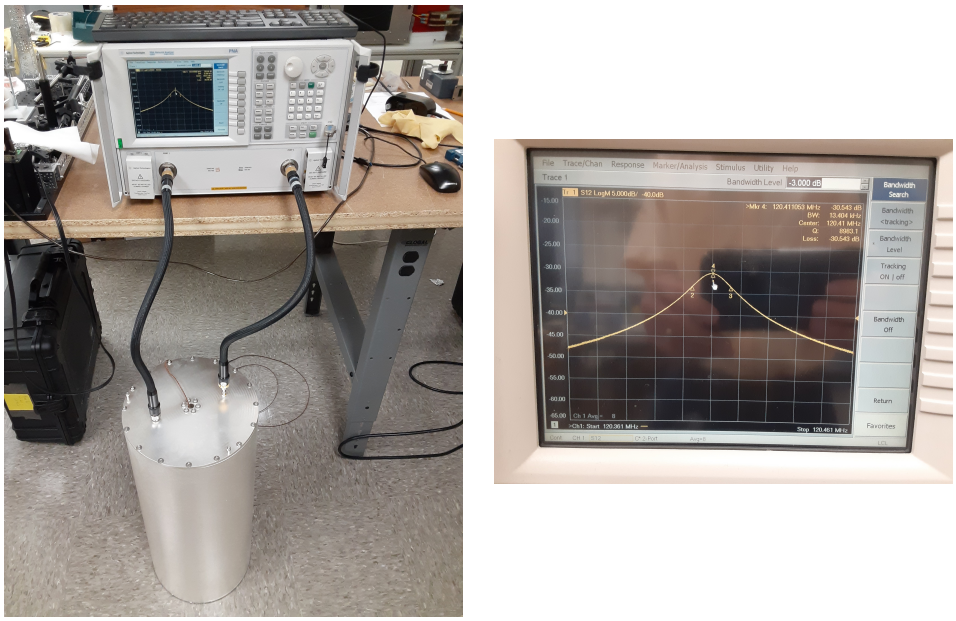

Figure 10: Empty resonator measurements for simulation model calibration.

Table 4: Empty resonator measured values and simulated values based on measured dimensions and corrected dimensions.

	Meas. Value	Uncorr. Sim. Value	Corr. Sim. Value
Frequency [MHz]	120.436	120.432	120.436
Q	8777.0	9825.1	8777.3
Loss [dB]	-24.051	-	-

7 Ferroelectric Tube Measurements Near 80 MHz

The length and outer diameter of each tube were measured with a micrometer and the inner diameter with a caliper. Each measurement was made at at least three positions; the values are listed in Table 5. The difference in the average values for the outer and inner diameters between the two tubes are 0.020 and 0.059 mm, respectively.

Each ferroelectric tube was cleaned using the steps outlined above prior to measurement. To ensure good contact between the tube and metal surfaces, thin (0.004 inch, 0.102 mm) copper foil was cut into disks that fit within the counterbore on the bottom plate. One layer of foil was added at a time until

the measured quality factor was a consistent value; a single layer was sufficient for this. Figure 11 shows photos of the foil and tube in the resonator.

Table 5: The dimensions of each ferroelectric tube.

	Measurement [mm]	Average [mm]
Tube 1 length	31.803	
	31.793	
	31.808	31.802
Tube 1 OD	26.998	
	26.995	
	26.998	
	26.990	26.995
Tube 1 ID	16.840	
	16.878	
	16.878	16.866
Tube 2 length	31.780	
	31.801	
	31.803	31.795
Tube 2 OD	27.015	
	27.015	
	27.013	
	27.018	27.015
Tube 2 ID	16.929	
	16.929	
	16.916	16.925

The procedure for measuring the tubes is as follows: place a fresh copper foil in the bottom plate counterbore; place the tube in the center of the bottom plate counterbore; replace the top plate; tighten the screws of the top plate; connect the Agilent Technologies PNA Network Analyzer Model E8362C; wait $\geq$15 minutes for the temperature of the tube to equilibrate; record the data; remove the top plate; remove the tube. New foil was used for each subsequent measurement. This procedure was repeated at least three times for each of the two tubes.

Tables 6 and 7 list the data for the lowest order mode for each ferroelectric tube. The foil for Tube 2 was not replaced for Trial 2, which caused the quality factor to be lower than the rest of the measurements.

8 Sources of Uncertainty

There are several sources of uncertainty that contribute to the error reported in the dielectric constant and loss tangent in the next section. These include: asymmetry in the outer conductor, uncertainty in the resonator length, manu-

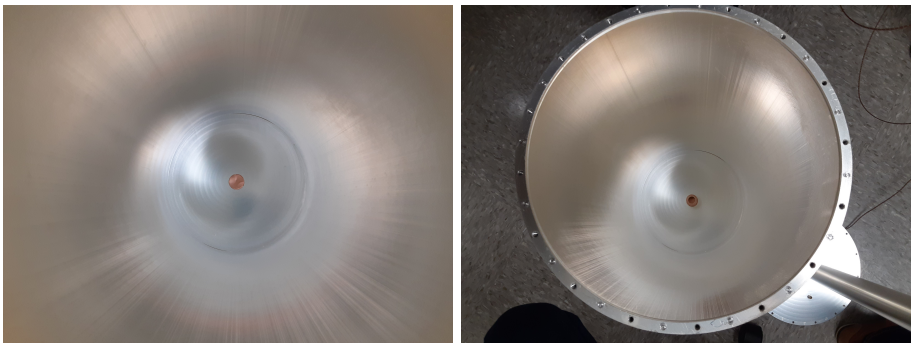

Figure 11: Photos of the copper foil disks placed in the bottom plate counterbore (left) and the ferroelectric tube placed on the foil (right).

Table 6: Data for the lowest order mode of ferroelectric Tube 1.

	Trial 1	Trial 2	Trial 3	Trial 4
Frequency [MHz]	69.936	70.029	70.061	70.370
Q	2831.9	2810.1	2854.9	2855.6
Loss [dB]	-45.670	-45.611	-45.445	-45.928
Measured Temp. [C]	20.7	21.1	21.2	21.9
Calibrated Temp. [C]	20.9	21.2	21.4	22.1

Table 7: Data for the lowest order mode of ferroelectric Tube 2.

	Trial 1	Trial 2	Trial 3	Trial 4
Frequency [MHz]	70.138	70.198	70.233	70.314
Q	2808.8	2415.5	2866.8	2772.0
Loss [dB]	-45.720	-47.186	-45.632	-45.779
Measured Temp. [C]	21.3	21.5	21.7	21.9
Calibrated Temp. [C]	21.5	21.7	21.9	22.1

facturing imperfections in the ferroelectric tube length and diameter, and uncertainty in the effective conductivity of the resonator.

As noted previously, the outer conductor is not a perfectly circular cylinder: the bottom is more elliptical than the top, based on the measurements listed in Table 3. This does not affect the results of the lowest order mode significantly, as shown in Figure 12. The calculated dielectric constant of the lowest order mode is 159.5 for a circular cylinder and 159.1 for an elliptical cylinder, a 0.25% difference.

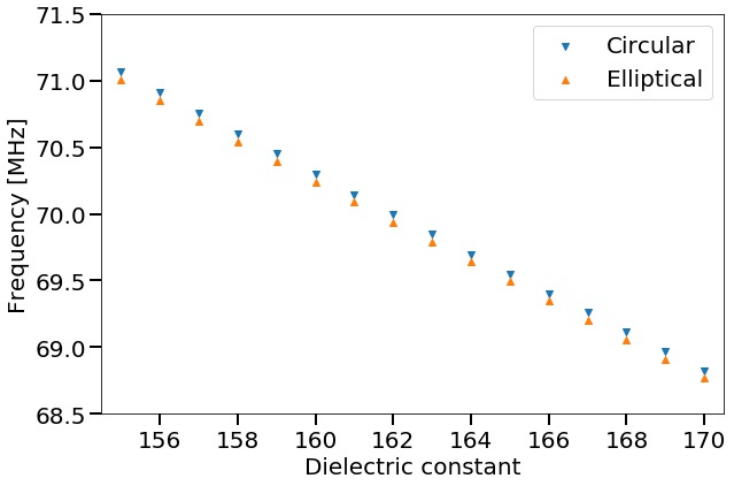

Figure 12: Simulated frequency vs. ferroelectric tube dielectric constant for the case of a perfectly circular cylinder and an elliptical cylinder.

The largest source of uncertainty is the resonator length, which is a combination of manufacturing and measurement error in the outer conductor length and turndown depths for the outer conductor and top and bottom plates. The measured value, based on the dimensions in Table 3, is 604.95 mm, and the corrected value, based on the simulation of the empty structure, is 603.652 mm. Figure 13 shows the calculated dielectric constant as a function of resonator length. The vertical lines are at the calibrated resonator length based on the resonant frequency of the empty structure (red) and the measured resonator length (magenta). The difference between the calculated dielectric constant for the calibrated resonator length, 159.1, and the measured resonator length, 158.5, is 0.38%. The difference in resonator length between the measured and calibrated values does not affect the calculated loss tangent of the ferroelectric tube.

The measured length of Tube 1 varied by 0.015 mm (see Table 5). Figure 14 shows the calculated dielectric constant as a function of ferroelectric tube length. The vertical lines are at the average value of the measured tube lengths, 31.802 mm, and the minimum measured value, 31.793 mm. The calculated dielectric constant for the average measured tube length is 159.14 and for the minimum

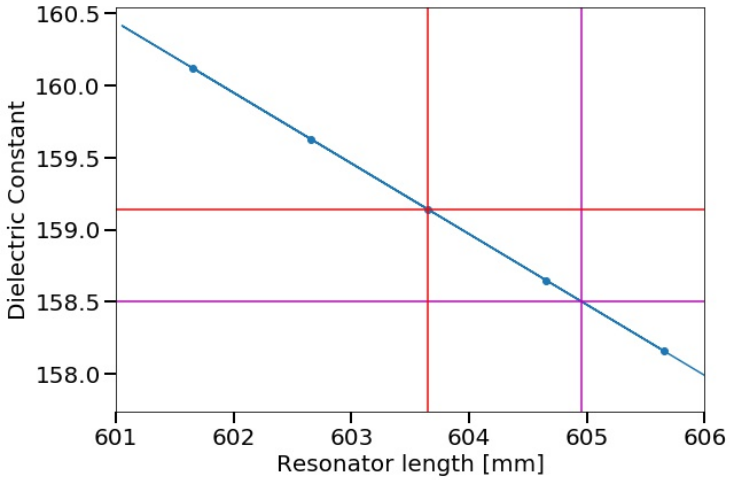

Figure 13: Calculated dielectric constant of the ferroelectric tube vs. resonator length. The red lines correspond to the calibrated resonator length and the magenta lines to the measured resonator length.

measured tube length is 159.09, a difference of 0.03%. This small variation is negligible compared to the other sources of uncertainty. The difference in measured values of ferroelectric tube length does not affect the calculated loss tangent of the tube.

The measured inner diameter of Tube 1 varied by 0.038 mm. Figure 15 shows the calculated dielectric constant as a function of ferroelectric tube inner diameter. The vertical lines are at the average value of the measured inner diameter, 16.866 mm, and the minimum measured value, 16.840 mm. The calculated dielectric constant for the average measured tube inner diameter is 159.1 and for the minimum measured inner diameter is 158.8, a difference of 0.19%. The difference in measured values of the ferroelectric tube inner diameter does not affect the calculated loss tangent of the tube.

The calculated loss tangent of the ferroelectric tubes is dependent on the surface conductivity in the simulation model. The loss tangent is in general not dependent on ferroelectric temperature (see the results in the next section). The spread in measured values of the quality factor for the two ferroelectric tubes is on the order of 2-3% (see Tables 6 and 7). A 3% variation in the quality factor of the empty resonator results in ≈6% difference in the effective surface conductivity. Figure 16 shows the calculated loss tangent as a function of resonator surface conductivity. The vertical lines correspond to the calibrated surface conductivity, 49.15×10^6 S/m, and a 6% larger value. The calculated loss tangent for the calibrated surface conductivity is 2.97×10^{-4}, which increases to 3.03×10^{-4} for a 6% larger conductivity, a difference of 2%.

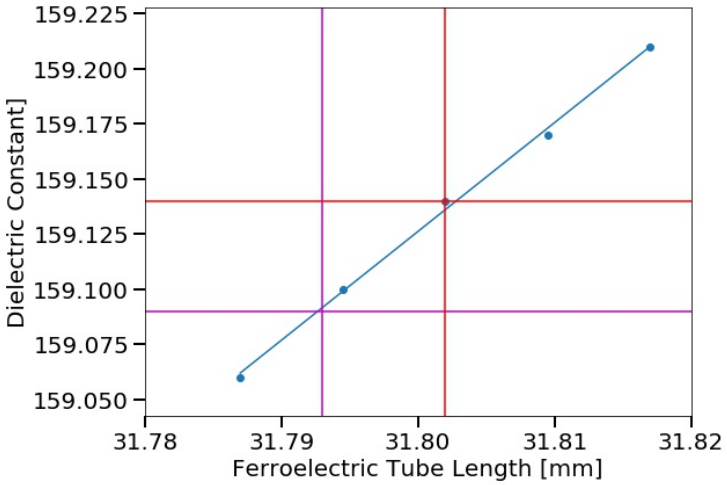

Figure 14: Calculated dielectric constant of the ferroelectric tube vs. tube length. The red lines correspond to the average of the measured lengths and the magenta lines correspond to the minimum measured value.

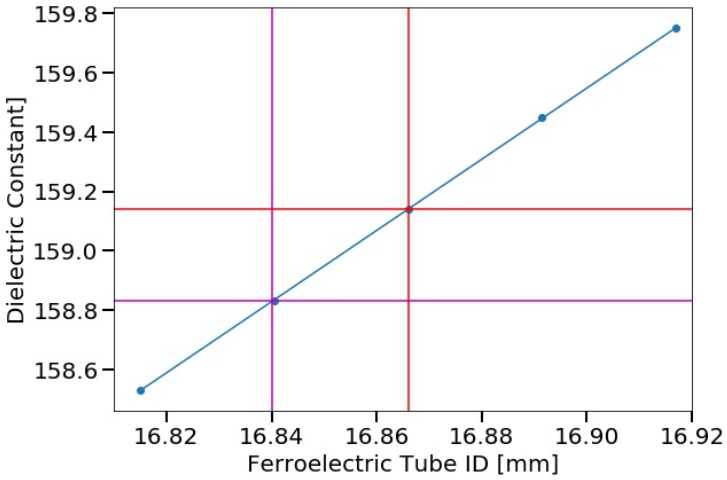

Figure 15: Calculated dielectric constant of the ferroelectric tube vs. tube inner diameter. The red lines correspond to the average of the measured diameters and the magenta lines correspond to the minimum measured value.

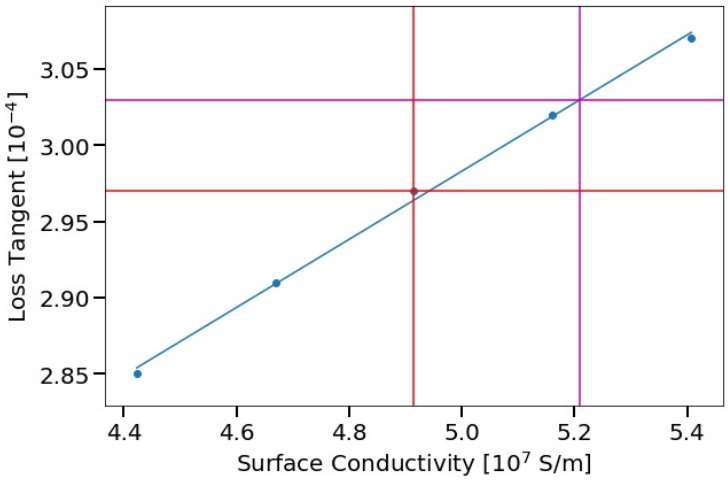

Figure 16: Calculated ferroelectric loss tangent vs. resonator surface conductivity. The red lines correspond to the calibrated surface conductivity and the magenta lines to the surface conductivity based on the spread in quality factor of the ferroelectric tube measurements.

9 Dielectric Constant and Loss Tangent Results

To determine the dielectric constant of each ferroelectric tube, the resonant frequency was simulated over a range of dielectric constants; the dielectric constant that resulted in a simulated frequency that matched the measured frequency was selected. The loss tangent was determined in a similar manner: once the dielectric constant was calculated, a parameter sweep of the loss tangent was performed and the loss tangent that resulted in the measured quality factor selected. The calculated dielectric constants and loss tangents of the lowest order mode for each tube are listed in Table 8. The uncertainty for each measurement was determined by adding the individual sources discussed above in quadrature. For the dielectric constants, the uncertainty is 0.367%, or ± 0.6 for all trials. For the loss tangents, the uncertainty is 2%, or $\pm 0.06 \times 10^{-4}$ for all trials. As noted above, the values for Trial 2 for Tube 2 are a result of a used copper foil. It can be seen that the contact between the ceramic and metal affects the loss tangent on the order of 25%.

The results from Table 8 are plotted in Figures 17 and 18. The dielectric constant is very clearly dependent on temperature, while the loss tangent is independent. The temperature dependence of the dielectric constant is fairly consistent between the two tubes. The measurements at 22.1°C differ in dielectric constant by 0.375% between the two tubes, consistent with the measurement uncertainty. Discounting the compromised data point for tube 2, the average loss tangent for tube 1 is 2.99×10^{-4} with a standard deviation of 3.42×10^{-6}, and for tube 2 is 3.03×10^{-4} with a standard deviation of 9.02×10^{-6}. Combining

Table 8: Lowest order mode calculated values for the dielectric constant and loss tangent for each measurement for each ferroelectric tube. The uncertainty in the measured dielectric constant is ± 0.6 and $\pm 0.06 \times 10^{-4}$ in the loss tangent. The calibrated temperature at which the measurement was made is also given.

	Trial 1	Trial 2	Trial 3	Trial 4
Tube 1 ϵ_r	162.0	161.4	161.2	159.1
Tube 1 $\tan\delta$ $[10^{-4}]$	2.99	3.03	2.95	2.97
Tube 1 temperature [C]	20.9	21.3	21.4	22.1
Tube 2 ϵ_r	161.0	160.6	160.3	159.8
Tube 2 $\tan\delta$ $[10^{-4}]$	3.04	3.86	2.94	3.12
Tube 2 temperature [C]	21.5	21.7	21.9	22.1

the two tube results, the average loss tangent is 3.01×10^{-4} and the standard deviation is 6.29×10^{-6}.

Fitting the dielectric constant as a function of temperature with a linear fit, the dielectric constant of this ferroelectric material is 159.9 ± 0.6 at 22° C. Including the systematic and statistical uncertainty, the value of the loss tangent is $(3.01 \pm 0.12) \times 10^{-4}$.

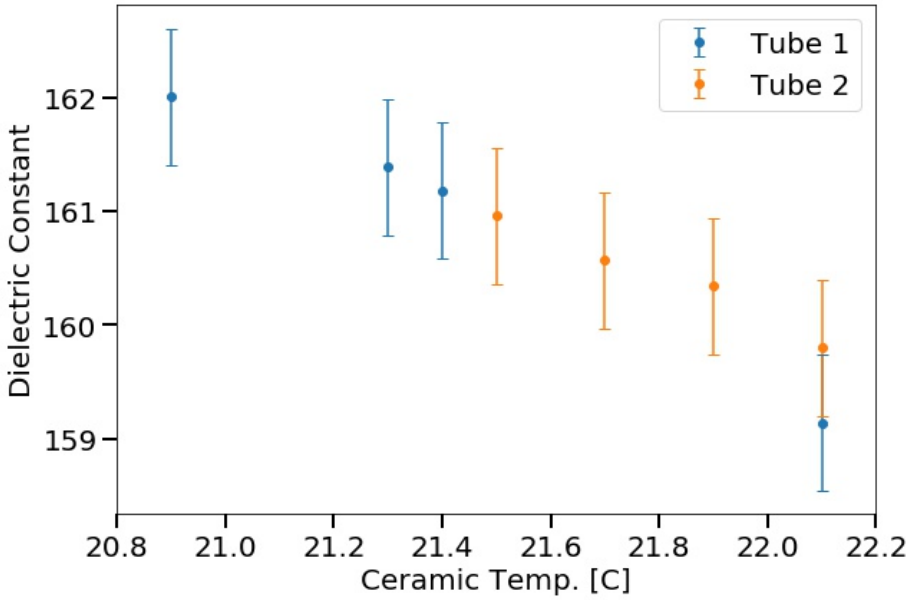

Figure 17: Dielectric constant vs. ceramic temperature for the two ferroelectric tubes.

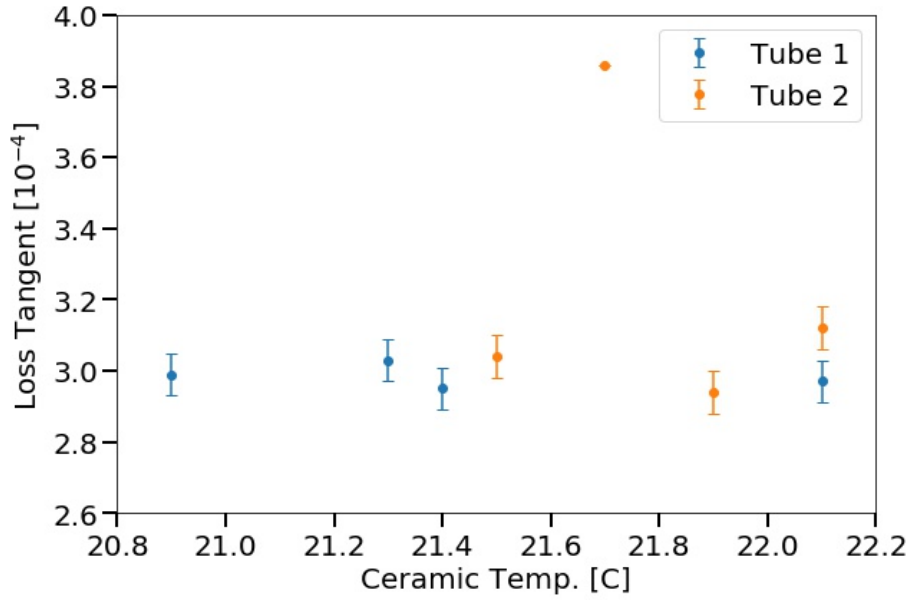

Figure 18: Loss tangent vs. ceramic temperature for the two ferroelectric tubes. The large value for Tube 2 near 21.7°C is a result of the copper foil not being replaced for that measurement.

A Appendix: Higher Order Modes

There are several higher order modes less than 1 GHz. Each of these was measured once for each tube; the results are given in Tables 9 and 10.

Table 9: Measured values for the higher order modes for Tube 1.

Freq. [MHz]	Q	Loss [dB]	Meas. Temp. [C]	Cal. Temp. [C]
269.626	4590.5	-28.289	21.8	22.0
503.397	7013.3	-22.922	21.4	21.6
700.918	6837.7	-36.947	21.5	21.7
703.631	6037.7	-61.150	21.5	21.7
744.482	7332.2	-23.502	21.6	21.8
826.755	11488	-22.801	21.6	21.8
829.020	6727.9	-49.978	21.7	21.9
987.706	3788.2	-31.245	21.8	22.0
994.173	17799	-16.232	21.8	22.0

Table 10: Measured values for the higher order modes for Tube 2.

Freq. [MHz]	Q	Loss [dB]	Meas. Temp. [C]	Cal. Temp. [C]
269.677	4255.5	-28.962	22.0	22.2
503.462	6240.1	-23.901	22.0	22.2
700.988	7318.3	-39.003	22.2	22.4
703.617	6816.5	-46.348	22.2	22.4
744.497	6952.7	-23.240	22.2	22.4
826.795	10793	-25.774	22.4	22.6
829.063	5135.0	-39.894	22.3	22.5
987.908	7081.7	-25.867	22.2	22.4
994.200	18373	-18.803	22.2	22.4
996.177	4986.6	-36.961	22.2	22.4

The elliptical geometry of the outer conductor results in several degenerate modes separating due to the asymmetry in the x and y dimesions. Figure 19 shows the simulated results of two modes that are degenerate for a circular cylinder, but separate for the existing elliptical cylinder.

The calculated dielectric constant of the second mode of the resonator (first higher order mode listed in Tables 9 and 10, f$\sim$270 MHz) is 160.3$\pm$0.6 for both ferroelectric tubes (Tube 1 at 22.0°C, Tube 2 at 22.2°C). This value is consistent with the lowest order mode, plotted in Figure 17. The calculated loss tangent of the second mode is (9.09$\pm$0.18) $\times 10^{-4}$. Previous measurements of this ferroelectric material indicate the loss tangent is 8×10^{-4} at 750 MHz [7], 3-4$\times10^{-3}$ at 3.5 GHz [8], and 4-5$\times10^{-3}$ at 10 GHz [1, 9, 10].

Beginning with the third mode of the resonator, f$\sim$500 MHz, the asymmetry

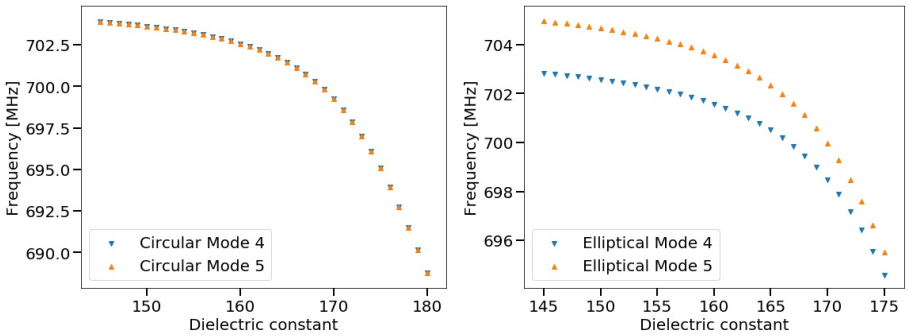

Figure 19: Simulated frequency vs. ferroelectric tube dielectric constant. For a perfectly circular outer conductor, the fourth and fifth modes are degenerate - left. For the existing elliptical outer conductor, the two modes shift apart in frequency - right.

in the outer conductor and inability to precisely model it invalidated the simulation results. For measurements of the dielectric properties of this ferroelectric material at high frequencies, a resonator designed for that purpose is required to provide accurate results.

B Appendix: Mechanical Drawings

All mechanical drawings are provided here.

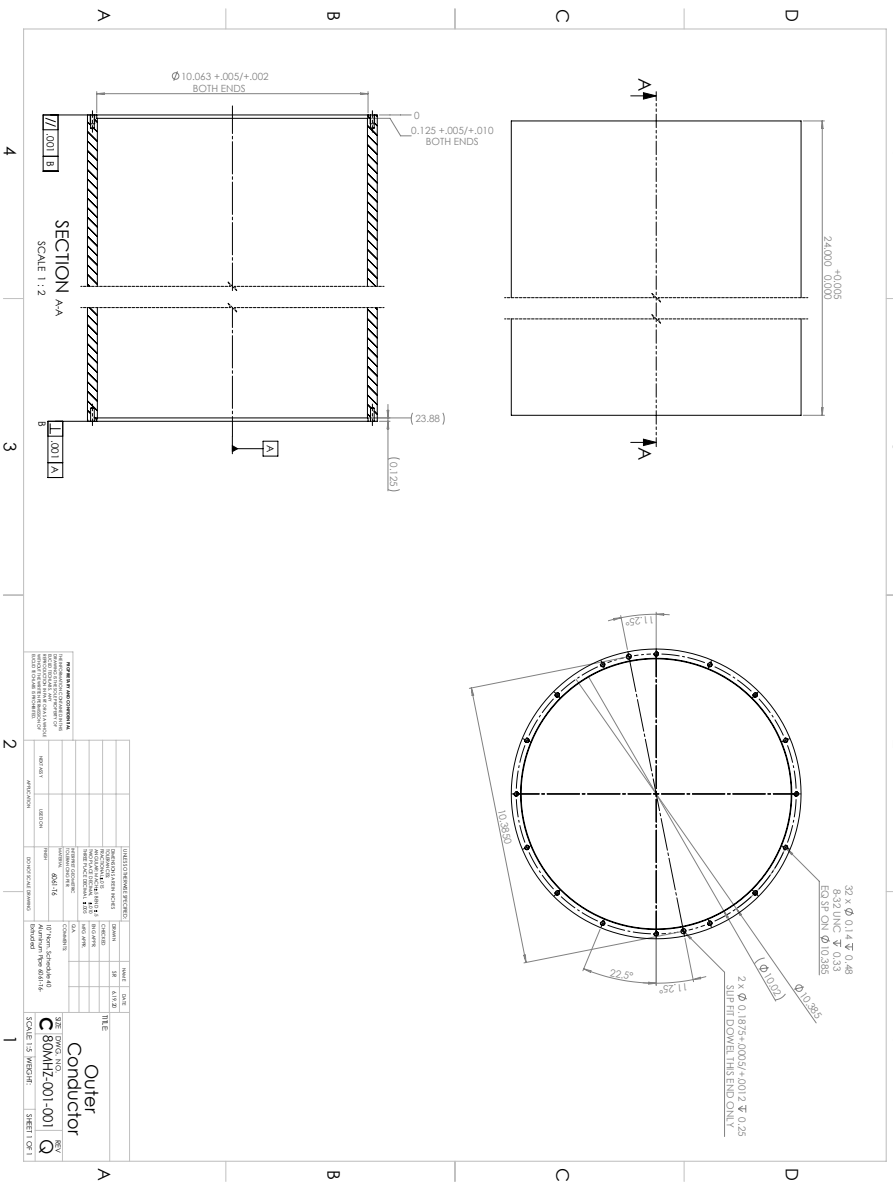

Figure 20: Outer conductor.

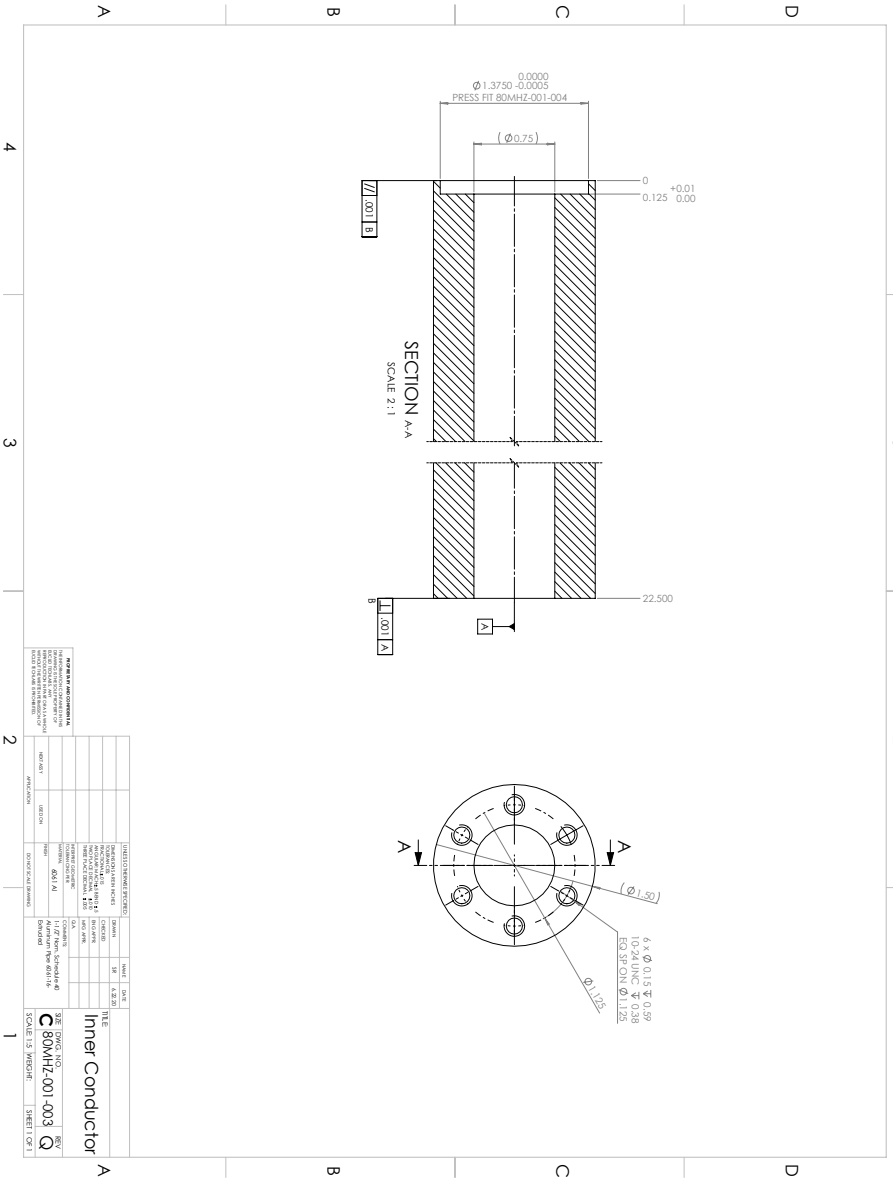

Figure 21: Inner conductor.

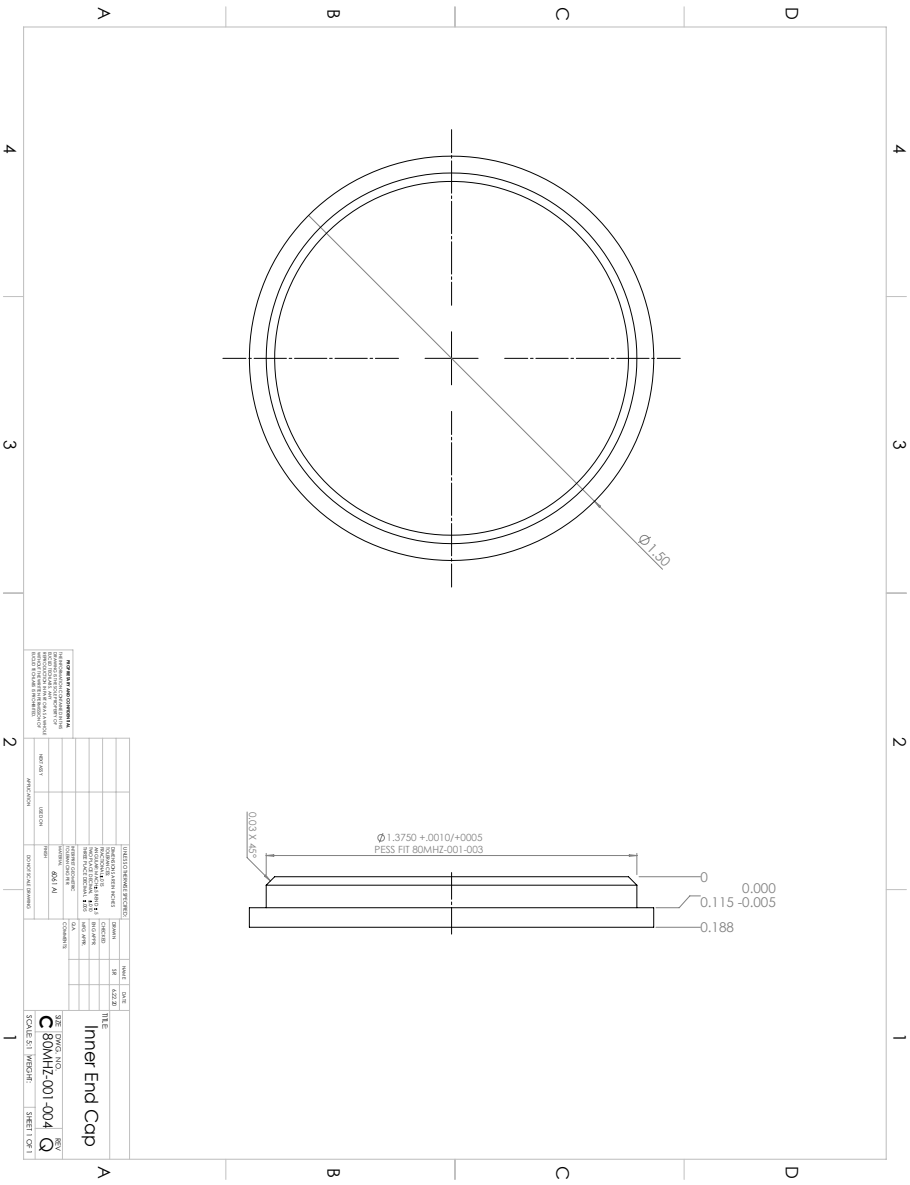

Figure 22: Inner conductor end cap.

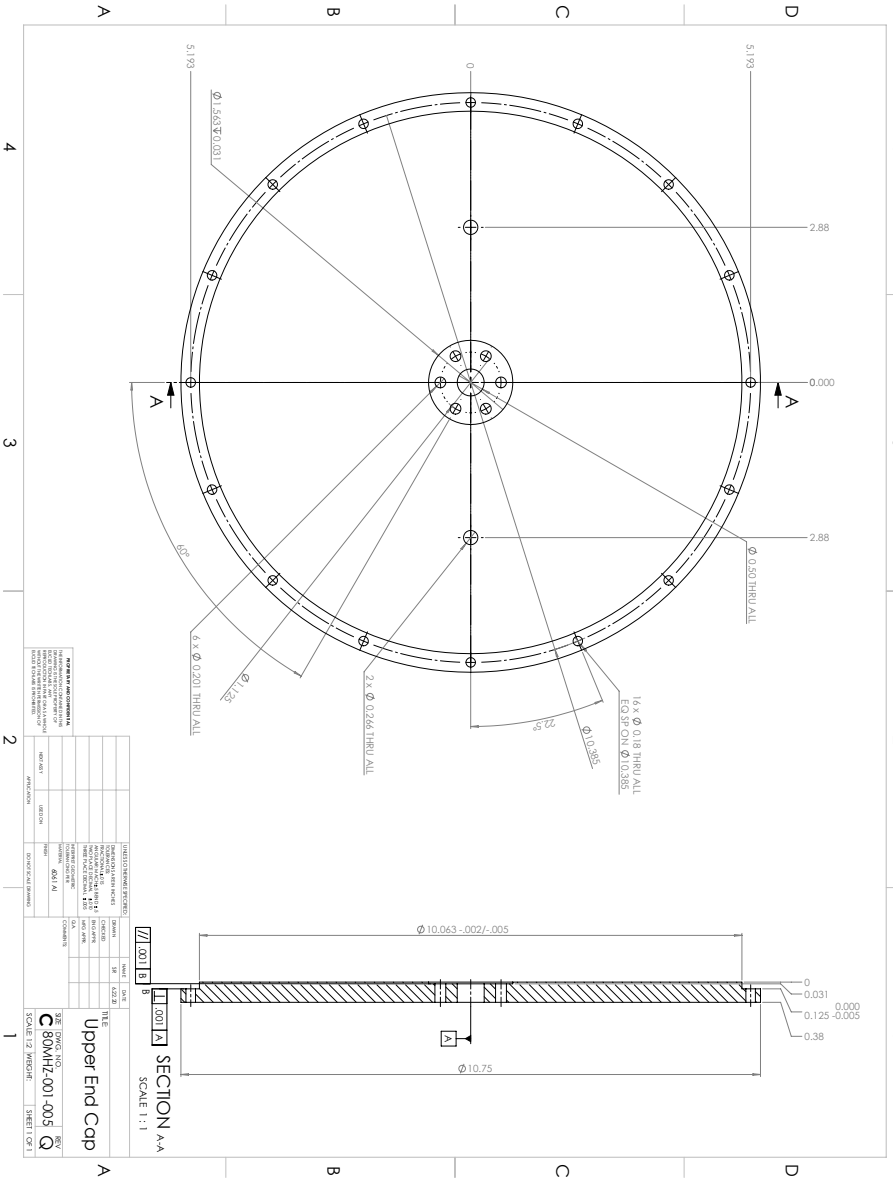

Figure 23: Top plate.

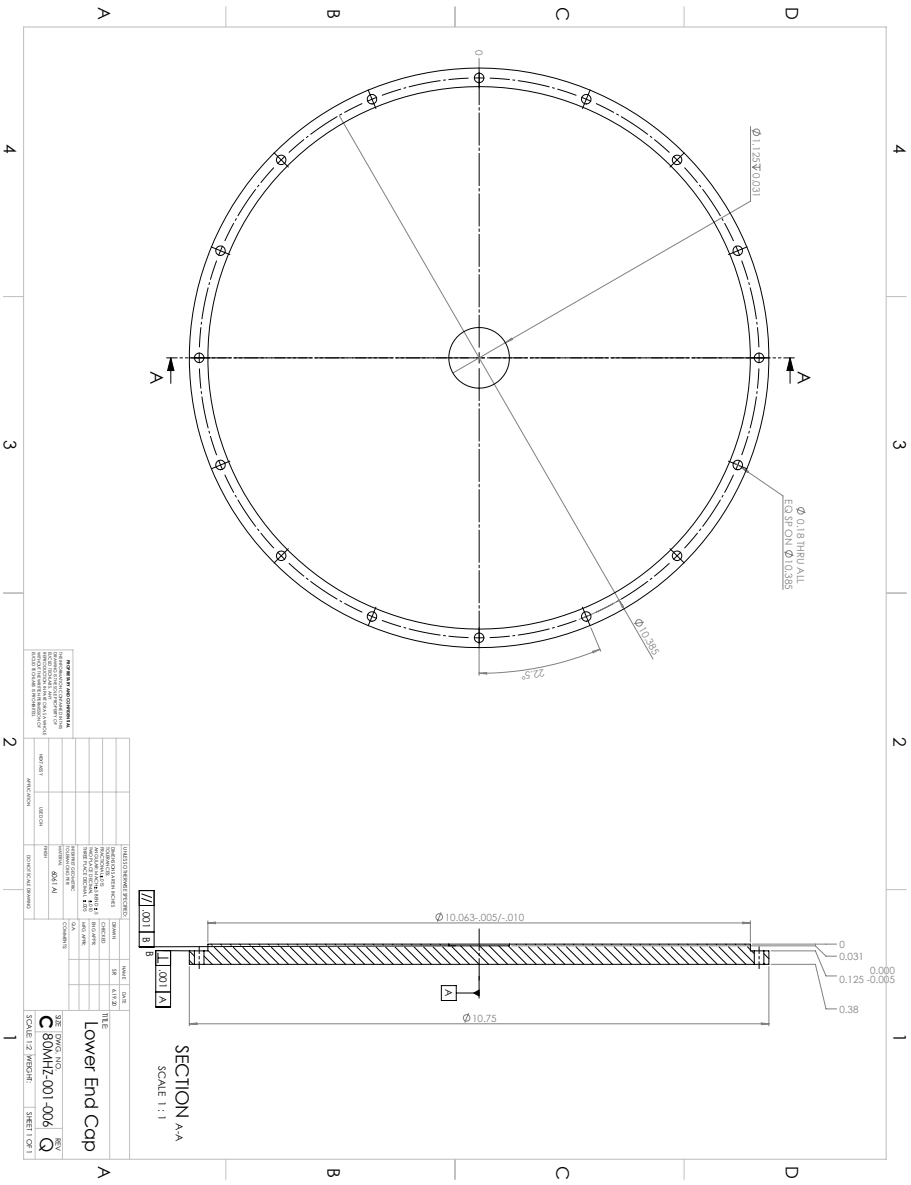

Figure 24: Bottom plate.

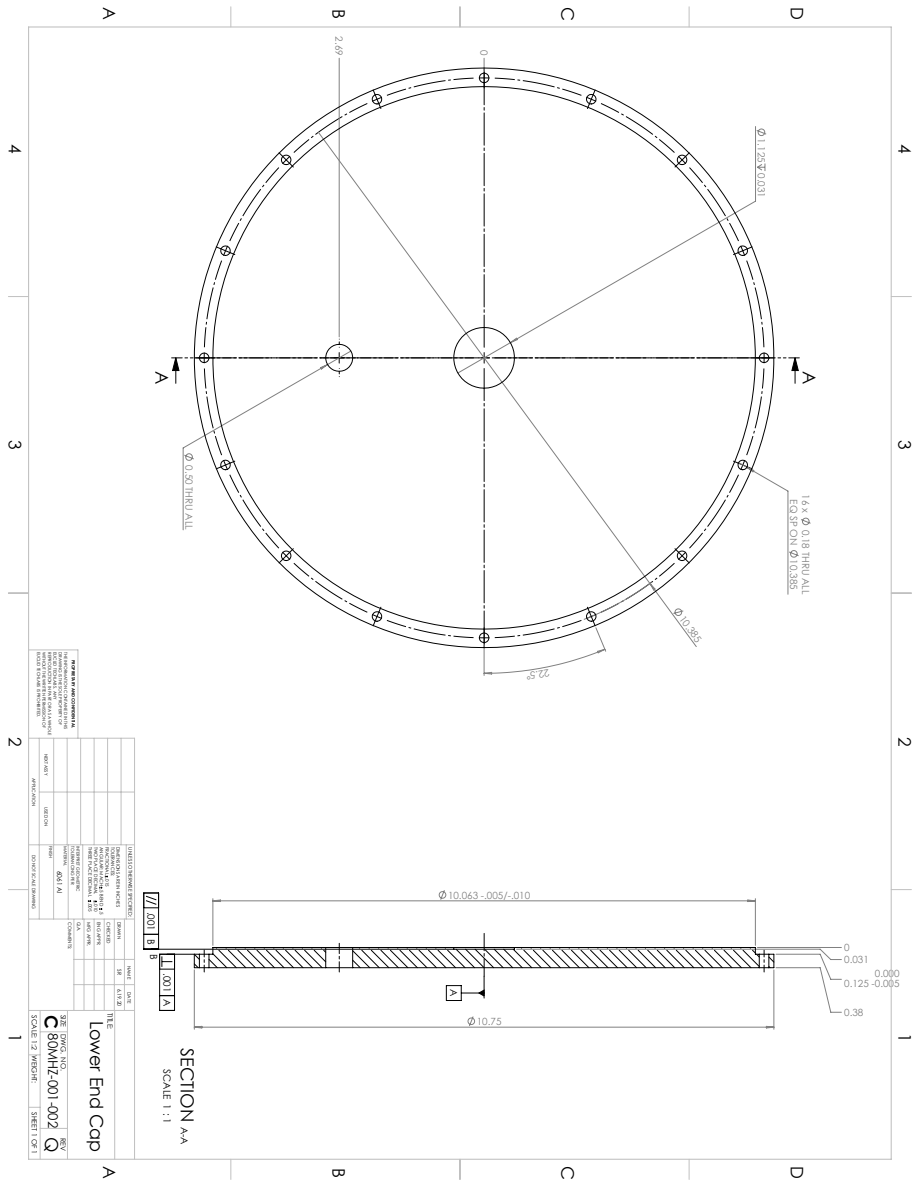

Figure 25: Bottom plate with penetration for thermocouple.

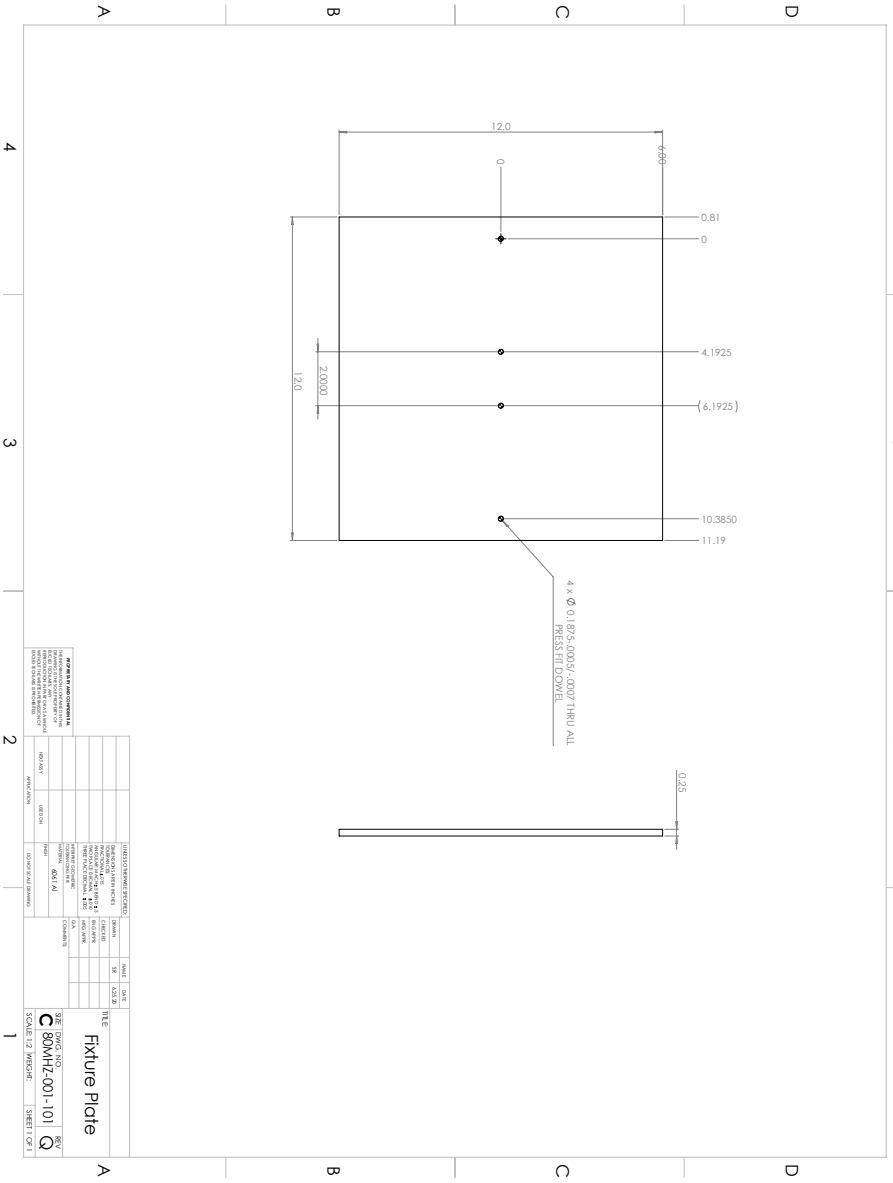

Figure 26: Alignment fixture plate.

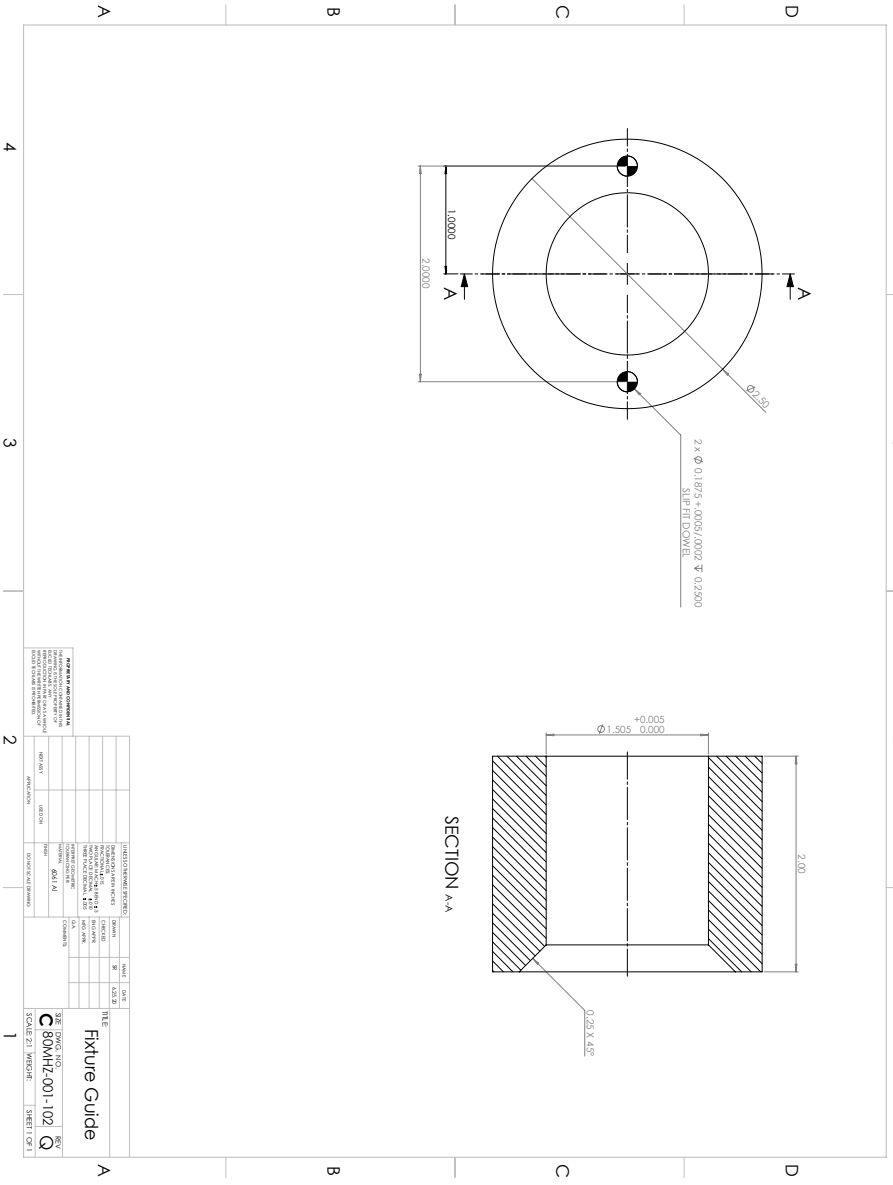

Figure 27: Alignment fixture.

References

[1] N. Shipman et al. A ferroelectric fast reactive tuner for superconducting cavities. In *Proceedings of SRF 2019*, pages 781–788, 2019. doi: 10.18429/JACoW-SRF2019-WETEB7.

[2] Online Metals. 10" nom. schedule 40 aluminum pipe 6061-t6-extruded. URL `https://www.onlinemetals.com/`.

[3] Xometry. URL `www.xometry.com`.

[4] Nobert Plating Co. URL `www.nobertplating.com`.

[5] McMaster-Carr. Thermocouple probe for surfaces; nickel probe, 12 feet long cable. URL `www.mcmaster.com/9251T74`.

[6] L. G. Hector and H. L. Schultz. The dielectric constant of air at radiofrequencies. *Physics*, 7(4):133–136, 1936. doi: 10.1063/1.1745374. URL `https://doi.org/10.1063/1.1745374`.

[7] C. Jing et al. Dielectric measurements of ferroelectric ceramic tubes. Euclid Techlabs Technical Report, 2017.

[8] E.A. Nenasheva et al. Low permittivity ferroelectric composite ceramics for tunable applications. *Ferroelectrics*, 506:174–183, 2017. doi: 10.1080/00150193.2017.1282761. URL `http://dx.doi.org/10.1080/00150193.2017.1282761`.

[9] E.A. Nenasheva et al. Low loss microwave ferroelectric ceramics for high power tunable devices. *J. Eur. Cer. Soc.*, 30:395–400, 2010.

[10] A. Kanareykin et al. Ferroelectric based high power tuner for l-band accelerator applications. In *Proceedings of IPAC'13*, pages 2486–2488, 2013.